



## OPEN

SUBJECT AREAS:  
ALZHEIMER'S DISEASE  
NATURAL PRODUCTSReceived  
23 June 2014Accepted  
26 August 2014Published  
12 September 2014Correspondence and  
requests for materials  
should be addressed to  
W.S.Z. (zws@bnu.  
edu.cn)\* Current address:  
Department of  
Pharmacology &  
Toxicology and  
Higuchi Bioscience  
Center, School of  
Pharmacy, University  
of Kansas, Lawrence,  
KS 66047, USA.

# Notoginsenoside R1 increases neuronal excitability and ameliorates synaptic and memory dysfunction following amyloid elevation

Shijun Yan<sup>1,2\*</sup>, Zhi Li<sup>1,3,4</sup>, Hang Li<sup>1,3,4</sup>, Ottavio Arancio<sup>2</sup> & Wensheng Zhang<sup>1,3,4</sup>

<sup>1</sup>State Key Laboratory of Earth Surface Processes and Resource Ecology, Beijing Normal University, Beijing 100875, China, <sup>2</sup>Taub Institute for Research on Alzheimer's Disease and the Aging Brain, Department of Pathology and Cell Biology, Columbia University, New York, NY10032, USA, <sup>3</sup>Beijing Area Major Laboratory of Protection and Utilization of Traditional Chinese Medicine, Beijing Normal University, Beijing 100088, China, <sup>4</sup>Engineering Research Center of Natural Medicine, Ministry of Education, Beijing Normal University, Beijing 100088, China.

Neurodegeneration and synaptic dysfunction observed in Alzheimer's disease (AD) have been associated with progressive decrease in neuronal activity. Here, we investigated the effects of Notoginsenoside R1 (NTR1), a major saponin isolated from *Panax notoginseng*, on neuronal excitability and assessed the beneficial effects of NTR1 on synaptic and memory deficits under the A $\beta$ -enriched conditions *in vivo* and *in vitro*. We assessed the effects of NTR1 on neuronal excitability, membrane ion channel activity, and synaptic plasticity in acute hippocampal slices by combining electrophysiological extracellular and intracellular recording techniques. We found that NTR1 increased the membrane excitability of CA1 pyramidal neurons in hippocampal slices by lowering the spike threshold possibly through a mechanism involving in the inhibition of voltage-gated K<sup>+</sup> currents. In addition, NTR1 reversed A $\beta$ 1-42 oligomers-induced impairments in long term potentiation (LTP). Reducing spontaneous firing activity with 10 nM tetrodotoxin (TTX) abolished the protective effect of NTR1 against A $\beta$ -induced LTP impairment. Finally, oral administration of NTR1 improved the learning performance of the APP/PS1 mouse model of AD. Our work reveals a novel mechanism involving in modulation of cell strength, which contributes to the protective effects of NTR1 against A $\beta$  neurotoxicity.

Alzheimer's disease (AD) is the most common form of dementia worldwide. It is characterized by the presence of extracellular deposits of amyloid protein in senile plaques, and intracellular deposits of tau protein in neurofibrillary tangles. A key feature of the disease is represented by the progressive synaptic dismantling, impairment of neurotransmission and deficiency of neuronal network connections [see review<sup>1</sup> for detail]. Therefore, AD has been recognized as a synaptopathy<sup>2</sup>. Because of the synaptic failure hypothesis, studies have frequently concentrated on analysis of synaptic function and plasticity; most of these studies have been performed in hippocampus and cerebral cortex. By contrast, there is much less information concerning the intrinsic properties of neurons following  $\beta$ -amyloid (A $\beta$ ) peptides elevation or in AD brain<sup>3</sup>. Recent studies have uncovered significant alterations at the level of intrinsic excitability of single neurons in AD mouse models<sup>4-6</sup> or upon exposure to A $\beta$ <sup>7,8</sup>.

A reduction of intrinsic neuronal excitability has been found in the cerebellar cortex of APP/PS1 mice, in mouse dentate gyrus after application of synthetic A $\beta$ 1-42 oligomers<sup>7</sup>, and in hippocampal CA1 pyramidal neurons of 5XFAD mice<sup>3</sup>. In fact, AD patients have decreased neuronal activity in brain<sup>9-11</sup>. Furthermore, a decrease in neuronal activity was observed in 29% of cortical neurons in APP/PS1 mice. Clusters of hyperactive neurons were found exclusively near  $\beta$ -amyloid plaques, possibly due to a compensatory mechanism, aimed at re-establishing the synaptic connectivity altered by the synaptic loss<sup>12</sup>. Abnormal neuronal excitability contributes to the deficits in synaptic connectivity and hippocampal-based memory performance<sup>6,9</sup>. Therefore, modulation of the neuronal excitability represents a potential strategy for preventing the impairments of synaptic function and memory in AD brain. In support of this hypothesis, rotigotine, a dopamine agonist with high affinity for D3 and D2 receptors increased cortical excitability and restored central cholinergic transmission in AD patients<sup>13</sup>. In



another report, levetiracetam, an antiepileptic drug, reduced abnormal spike activity and reversed synaptic dysfunction and deficits in learning and memory in human amyloid precursor protein transgenic mice<sup>14</sup>. In addition, dietary omega-3 was found to improve learning performance of diabetic rats by upregulation of the excitability of CA1 pyramidal neurons<sup>15</sup>.

*Panax notoginseng* (Sanqi), a famous traditional Chinese herb medicine, has a long history of use in East Asian countries for the treatment of cardiovascular disease<sup>16,17</sup>. Notoginsenoside R1 (NTR1), chemically named C47H80O18 (Fig. 1), a major ingredient isolated from *Panax notoginseng* roots<sup>18</sup>, is known to possess anti-inflammatory, anti-oxidative and anti-ischemia-reperfusion injury properties<sup>19–21</sup>. NTR1 is specifically distributed in *Panax notoginseng*, unlike other ginsenosides such as ginsenoside R1, Rg1, R3, etc., which are distributed in both *Panax notoginseng* and *Panax ginseng*. NTR1 has the same chemical structure as ginsenosides such as Rg1, Rb1, Rg2, and Rg3, a common four-ring hydrophobic steroid-like structure attached with sugar moieties<sup>22</sup>. Recent studies have shown that ginsenosides have multifaceted neuroprotective effects in AD and related models both *in vitro* and *in vivo*. For example, Ginsenoside Rb1, Rg1, and Rg3 displayed protective effects against A $\beta$  production and aggregation through mechanisms possibly including reduction of APP expression, inhibition on  $\beta$ -secretase activity as well as stimulation of  $\alpha$ -secretase activity<sup>23–25</sup>. In addition, Rg1 and Rd prevented A $\beta$ -induced neurotoxicity such as mitochondrial dysfunction, tau hyperphosphorylation as well as neuronal death<sup>26–28</sup>. Furthermore, ginsenosides remarkably improved cognitive performance of AD patients and rodent models<sup>29–31</sup>. In contrast to the defined neuroprotective effects of ginsenosides, whether notoginsenoside R1 has neuroprotective effects and its mechanism of action remain elusive. Here, we investigated the modulation by NTR1 of intrinsic excitability of hippocampal pyramidal neurons and the putative neuroprotective effects of NTR1 against A $\beta$ 1–42 oligomers-induced synaptic dysfunction and memory deficits in primary cultured hippocampal neurons, in acute brain slice, and in a mouse model of AD. Our study reveals that NTR1 prevents A $\beta$ -induced synaptic dysfunction and improves hippocampal-based memory performance in an AD mouse model through a possible mechanism involved in the modulation of neuronal excitability.

## Results

**NTR1 increases membrane excitability of hippocampal CA1 pyramidal neurons.** Since neuronal excitability has been associated with synaptic plasticity, learning and memory<sup>32</sup> and a disturbance in

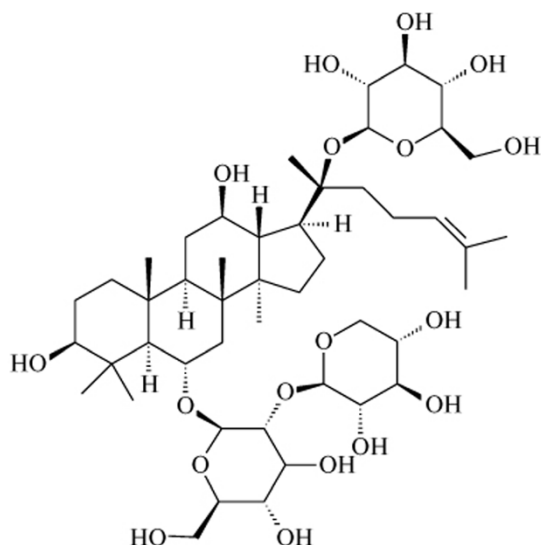


**Figure 1** | Chemical structure of notoginsenoside R1 (NTR1).

equilibrium between silent and hyperactive neurons has been shown in AD mouse brain<sup>12</sup>, we investigated the effects of NTR1 onto intrinsic excitability of pyramidal neurons in the hippocampal CA1 region, an area critically involved in memory formation. In coronal brain slices from mice of 2–3 months of age, spontaneous action potential (sAPs) of hippocampal CA1 pyramidal neurons were recorded without intermittency using the whole cell patch clamp technique. NTR1 at a concentration of 10  $\mu$ M was added to the perfusion system. After NTR1 perfusion for 20 min, NTR1 was washed out by switching the bath solution to normal ACSF. The spontaneous firing rate of pyramidal neurons was obviously increased after 10  $\mu$ M NTR1 application compared with time-matched control (vehicle) (Fig. 2a, b). Washout for 20 min abolished the effect of NTR1 on firing (Fig. 2a, b). The whole-cell recordings were performed continuously during vehicle or NTR1 perfusion procedure and firing frequency was measured at 1 min interval. NTR1 did not affect the resting membrane potential or the amplitude of sAPs (Fig. 2c), which indicated that NTR1 increased membrane excitability of hippocampal neurons without depolarization of cell membrane.

### NTR1 decreases the threshold for the action potential appearance.

Using current-clamp configuration, evoked action potentials (eAPs) were elicited through depolarizing current injection ranging from  $-50$  pA to  $+90$  pA in hippocampal pyramidal neurons (Fig. 3a). Evoked by a current of 10 pA and 30 pA amplitudes, the firing frequency of neurons was significantly ( $p = 0.014$  for 10 pA and  $p = 0.028$  for 30 pA,  $n = 12$ ) increased after NTR1 application (Fig. 3b). Before NTR1 application, only 16.7% neurons ( $n = 12$ ) were able to elicit eAPs with 10 pA current injection. But after NTR1 treatment, 83.3% neurons displayed eAPs with 10 pA current injection (Fig. 3c). The delivery of 30 pA current elicited eAPs in 83.3% neurons in the absence of NTR1, while all neurons ( $n = 12$ ) showed eAPs in the presence of NTR1 (Fig. 3d). Consistent with spontaneous firing, the effect of NTR1 on eAPs generation could be also abolished by NTR1 washout. In addition, there is no significant difference in maximum firing rate evoked by 90 pA current injection after NTR1 application. These results indicate that NTR1 reversibly increases neuronal excitability, possibly due to a reduction of spike threshold.

### NTR1 decreases spike threshold possibly through inhibiting sustained potassium currents.

Spike threshold was next measured directly using the peak of the derivative of the spontaneous action potential (Fig. 4a). NTR1 significantly and reversibly decreased AP threshold (Fig. 4b,  $p = 0.0026$ ,  $n = 9$  cells). An efflux of potassium during single action potential can hyperpolarize the cell and thus inhibit threshold from being reached. Thus, we next determined the effect of NTR1 on voltage-dependent K<sup>+</sup> currents. Voltage-activated K<sup>+</sup> currents were recorded as shown on Fig. 4d. The membrane was held at  $-70$  mV, and a 300 ms voltage step was applied up to a value of  $+50$  mV. NTR1 treatment significantly, but reversibly, decreased the sustained K<sup>+</sup> currents (Fig. 4e,  $p = 0.018$ ,  $n = 7$ ), which were measured at the end of the 300 ms pulse.

Fast afterhyperpolarization (AHP) is known to be involved in delaying the subsequent firing of action potentials<sup>4</sup>. Thus, we investigated the effects of NTR1 on AHP amplitude, which may interpret the rare effect of NTR1 on maximum firing rate. AHP amplitude was slightly higher after NTR1 perfusion ( $-1.94 \pm 0.32$  mV for NTR1 versus  $-1.69 \pm 0.29$  mV for baseline and  $-1.68 \pm 0.14$  mV for 20 min washout,  $n = 9$  cells, Fig. 4c; representative traces are shown in Fig. 4a). This finding is in the same direction as the effect of NTR1 on the maximum rate of firing. These findings suggest that inhibition of voltage-dependent K<sup>+</sup> current channel by NTR1 may be responsible for the increase in excitability of the hippocampal neurons.

**Effect of NTR1 is major at a cellular level.** The increase in spontaneous firing may be due to the alternation of presynaptic

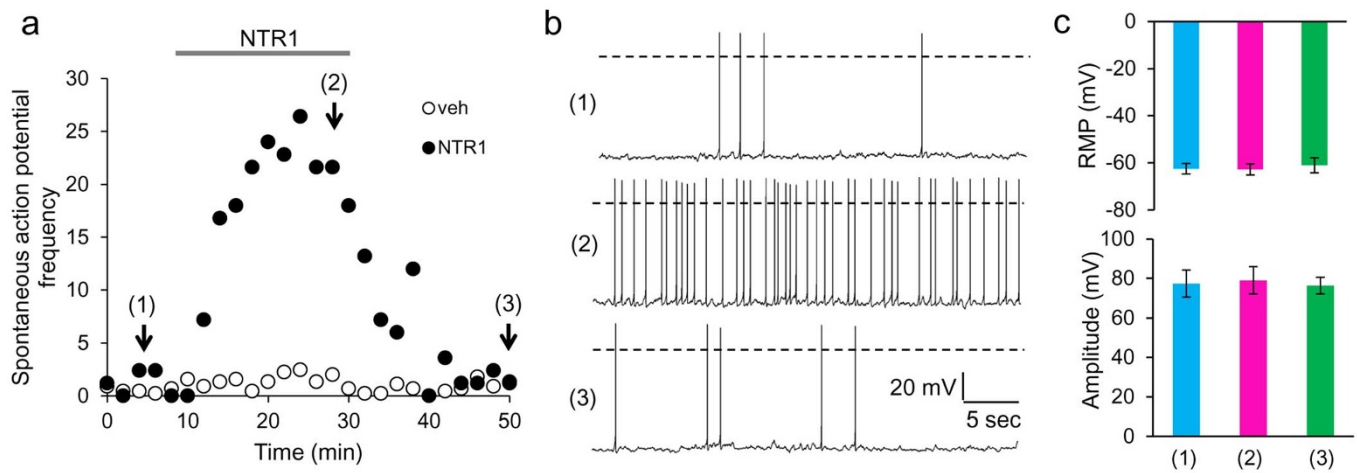


**Figure 2 | NTR1 enhances the excitability of hippocampal CA1 pyramidal neurons in acute brain slices.** (a). Changes in spontaneous action potentials (sAPs) frequency induced by NTR1 perfusion. sAPs frequency was measured at 1 min interval. (b). Representative traces of sAP firing in the same pyramidal neuron before NTR1 treatment (baseline, (1)), 20 min after 10  $\mu$ M NTR1 treatment (NTR1, (2)), and 20 min after washout (washout, (3)). (c). NTR1 did not affect resting membrane potential (upper) or sAPs amplitude (bottom) in pyramidal neurons.  $n=12$ .

transmission or the neuronal excitability, or both. To address this question, we recorded the spontaneous miniature excitatory postsynaptic currents (mEPSC), which can reflect any changes in presynaptic neurotransmitter release and postsynaptic receptor

activity and thus reflect the network changes<sup>33</sup>. mEPSCs were recorded in the presence of 100  $\mu$ M picrotoxin and 0.5  $\mu$ M TTX, which can exclude the effects of NTR1 on postsynaptic neuron properties but leave the synaptic response. No significance

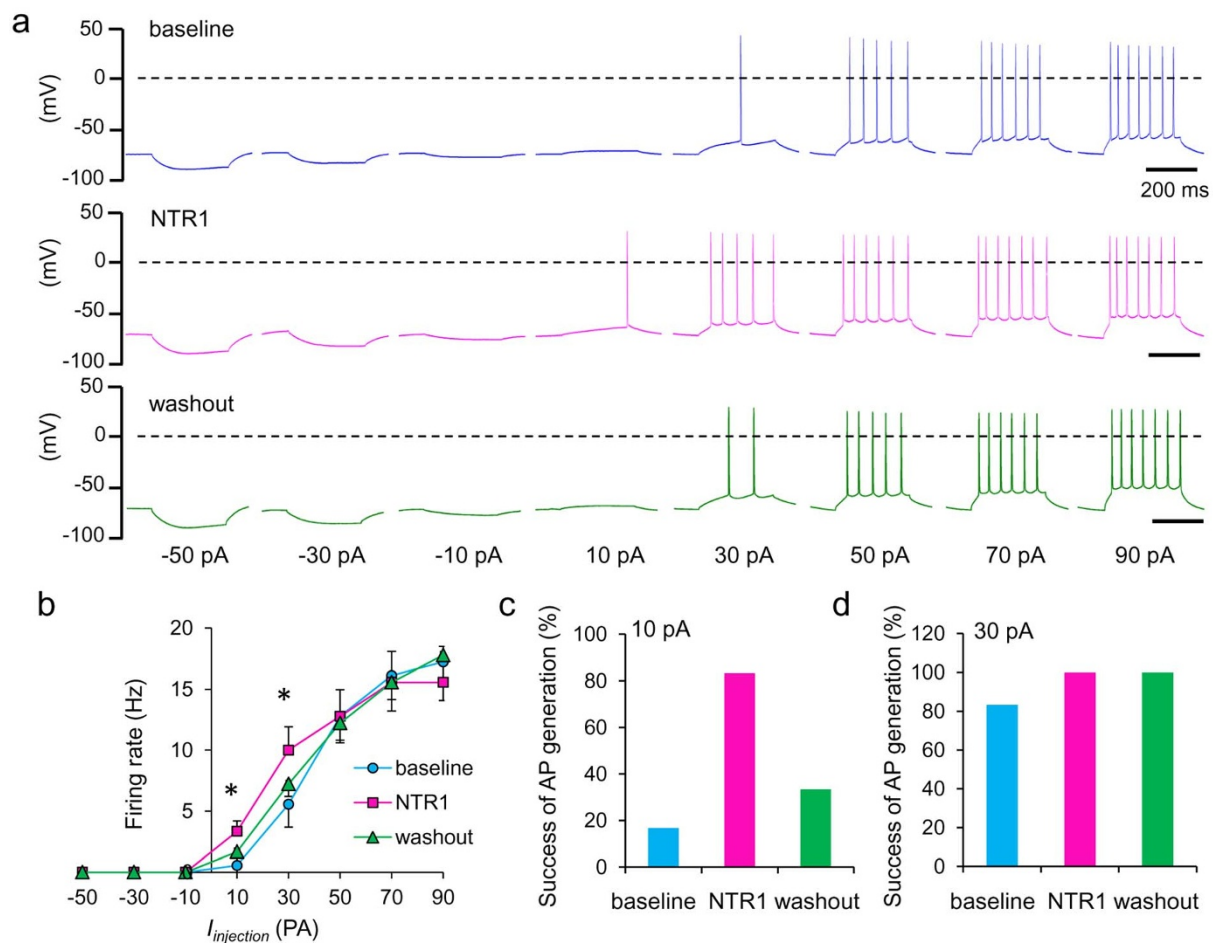


**Figure 3 | NTR1 decreases the AP threshold.** (a). Representative traces of membrane potential responding to step depolarization by current injection. Membrane potential was current-clamped at -70 mV; step depolarization was delivered by current injections with amplitudes ranging from -50 pA to 90 pA. (b). Frequency-current relationship of evoked action potential. (c). The percentage of neurons generating action potential by 10 pA current injection. (d). The percentage of neurons generating action potential by 30 pA current injection.  $n=12$ . \* $p < 0.05$ .

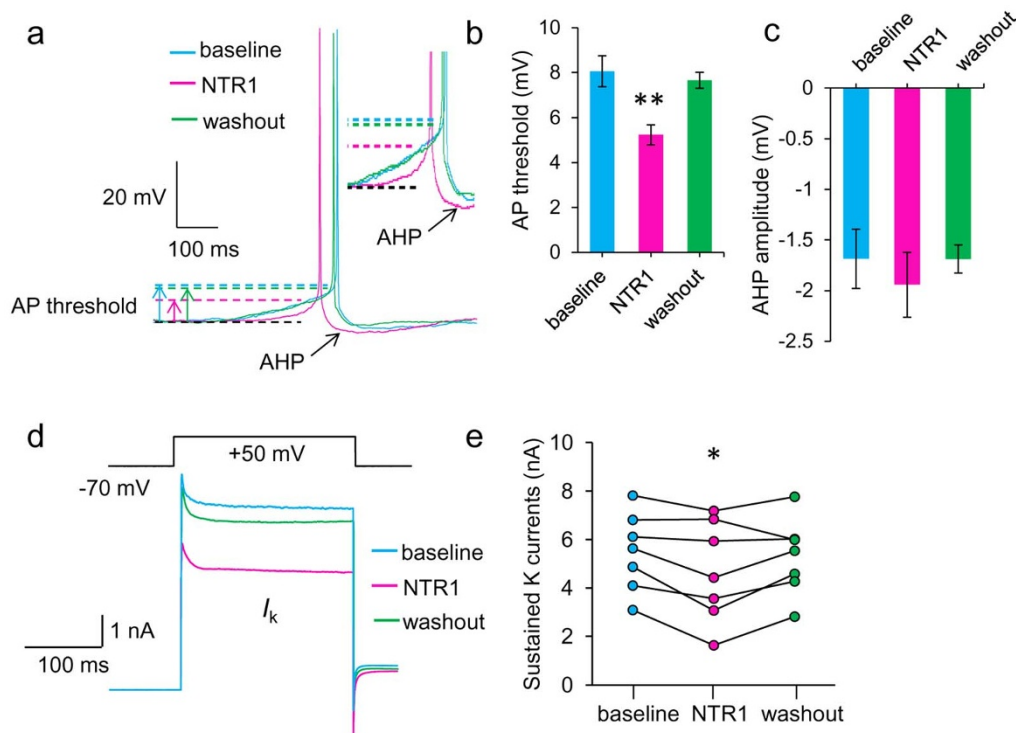


**Figure 4 | Effect of NTR1 on AP properties and voltage-gated  $K^+$  currents in hippocampal neurons.** (a). Representative traces of spontaneous action potential in the same CA1 pyramidal neuron before NTR1 application (baseline), in the presence of NTR1, and 20 min after NTR1 washout. The horizontal dotted lines represent the threshold and the resting membrane potential. Arrows indicate the negative peaks reached by the AHP. (b). Average of spike threshold.  $n=9$  cells. (c). Average of AHP amplitude, which are measured as the difference between resting membrane potential and AHP peak.  $n=9$  cells. (d). Representative voltage-gated  $K^+$  currents were evoked by delivering a voltage step to +50 mV in cells held at -70 mV. (e).  $K^+$  current quantification showed a reversible reduction of sustained  $K^+$  current in CA1 pyramidal neurons by NTR1 application ( $n=7$ ). Data from the same neuron were connected by lines. \* $p < 0.05$ , \*\* $p < 0.01$ .

difference was observed in mEPSC frequency (Fig. 5a, b) or amplitude (Fig. 5a, c) after NTR1 application. These findings suggest that the effect of NTR1 is major at a cellular level instead of a network based mechanism.

#### NTR1 rescues the LTP reduction induced by $A\beta$ 1-42 oligomers.

Changes in membrane excitability are known to be critical for memory formation<sup>34</sup> as the level of excitability within a network can reflect synaptic efficacy and plasticity<sup>32</sup>. In addition,  $A\beta$  elevation was able to reduce the neuron excitability *in vivo* and *in vitro*<sup>37</sup>. Therefore, we investigated the effects of NTR1 on  $A\beta$  oligomers-induced reduction of hippocampal long-term potentiation (LTP), a form of long-term synaptic plasticity. NTR1 alone didn't affect LTP in control condition ( $222.16 \pm 18.39\%$  for NTR1 alone versus  $228.59 \pm 10.50\%$  for vehicle-treated slices) (Fig. 6a, d).  $A\beta$ 1-42 oligomers (200 nM) perfusion significantly impaired LTP ( $152.49 \pm 6.50\%$  versus  $228.59 \pm 10.50\%$  for vehicle-treated slices,  $p < 0.001$ ) (Fig. 6b, d), which are consistent with previously reports<sup>35,36</sup>. NTR1 largely rescued the  $A\beta$ -induced reduction in LTP ( $213.19 \pm 9.36\%$ ,  $p < 0.001$ ) (Fig. 6c, d). Importantly, in the presence of 10 nM TTX which reduces the spontaneous firing activity, the protective effect of NTR1 against  $A\beta$ -induced LTP decline was completely abolished (Fig. 6c, d), suggesting that the protective effect of NTR1 on LTP is neuronal excitability-dependent. In our experiments, we did not find significant difference in basal neuronal synaptic transmission among all groups (Fig. 6e).

#### NTR1 rescues learning and memory deficits in an AD mouse model.

Spatial memory measured through the Morris Water Maze task is likely to be strongly dependent on neural activity in the CA1 sub-region of the hippocampus<sup>37,38</sup>. Therefore, we studied the effects of NTR1 on spatial memory in an  $A\beta$  deposition mouse model expressing

a chimeric human amyloid precursor protein (APP695swe) and a mutant human presenilin 1 (PS1-dE9) both directed to CNS neurons. After 4 months of NTR1 administration, the 7-month old animals were trained with the Morris Water Maze. All animals exhibited significant, substantial reductions in their times to find the platform over the training sessions (Fig. 7a). However, there were significant differences between APP/PS1 mice and WT mice ( $p = 0.025$ ). Compared to WT mice, 7-month old APP/PS1 took significantly longer time to find the platform occurring from the fourth-training day, implying a significant impairment of learning and memory. However, there were also significant differences between APP/PS1 mice treated with vehicle and those treated with NTR1 (Fig. 7a).

In the probe test, the platform was removed and the animal was released from the opposite quadrant. During the 60 sec of the probe trial, the number of crossings of APP/PS1 mice was significant less than WT control ( $1.75 \pm 0.53$  versus  $5.10 \pm 0.41$ ,  $n=10$ ,  $p < 0.001$ ). However, the number of crossings of the NTR1-treated APP/PS1 mice ( $3.33 \pm 0.33$ ,  $n = 8$ ) was significant more than the vehicle-treated APP/PS1 mice ( $p = 0.020$ ) (Fig. 7b, c). In addition, the APP/PS1 mice spent significant less time in the target quadrant compared to WT mice ( $15.86 \pm 1.99$  s versus  $30.14 \pm 1.68$ ,  $n=10$ ,  $p < 0.001$ ). However, the NTR1-treated APP/PS1 mice spent longer time in the target quadrant ( $24.11 \pm 2.22$ ,  $p = 0.015$ ), which was significant more than vehicle-treated APP/PS1 mice and similar to WT controls (Fig. 7d). There was no significant difference in swimming speed among all groups (Fig. 7e). These data indicate that NTR1 supplementation improves spatial learning and memory following  $A\beta$  elevation.

## Discussion

The neurodegeneration observed in AD has been associated with progressive decrease in neuronal activity and synaptic dismant-

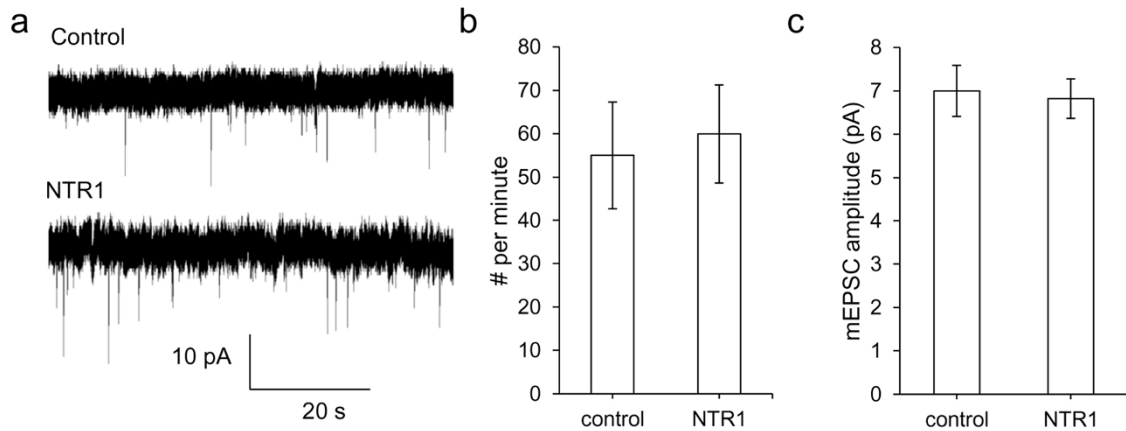


**Figure 5 | Effect of NTR1 on mEPSCs in hippocampal neurons.** (a). Representative recordings of mEPSCs in pyramidal neurons from acute slices in the presence or absence of 10  $\mu\text{M}$  NTR1. To isolate excitatory miniature events, 100  $\mu\text{M}$  picrotoxin and 0.5  $\mu\text{M}$  tetrodotoxin were added to the recording bath solution. (b). Average effect of NTR1 on mEPSCs frequency. (c). Average effect of NTR1 on mEPSCs amplitude.  $n=8$  cells.

ling<sup>9,10,39</sup>. Modulation of intrinsic properties of individual neurons represents a potential strategy for preventing and/or halting AD progression. Here, we found an increase in intrinsic excitability of hippocampal neurons by a natural compound, NTR1. Furthermore, our study is the first time to show that NTR1 prevented the A $\beta$ -induced synaptic plasticity deficits in brain slices and improved spatial learning and memory in an AD mouse model with a possible mechanism involving in neuronal excitability modulation.

A progressive decrease in neuronal activity was found in AD brains<sup>9–11</sup> and in mouse dentate gyrus following A $\beta$ 1–42 oligomers exposure<sup>7</sup>. Similarly in a study on 5XFAD mice, bearing five familial AD transgenes, A $\beta$ 1–42 production was associated with a reduction of membrane excitability in hippocampal CA1 pyramidal neurons<sup>3</sup>. However, several studies found neuronal hyperexcitability in the hippocampal-entorhinal cortex network in AD mice<sup>6,8,40</sup>. Busche MA and colleagues found a redistribution of synaptic drive between

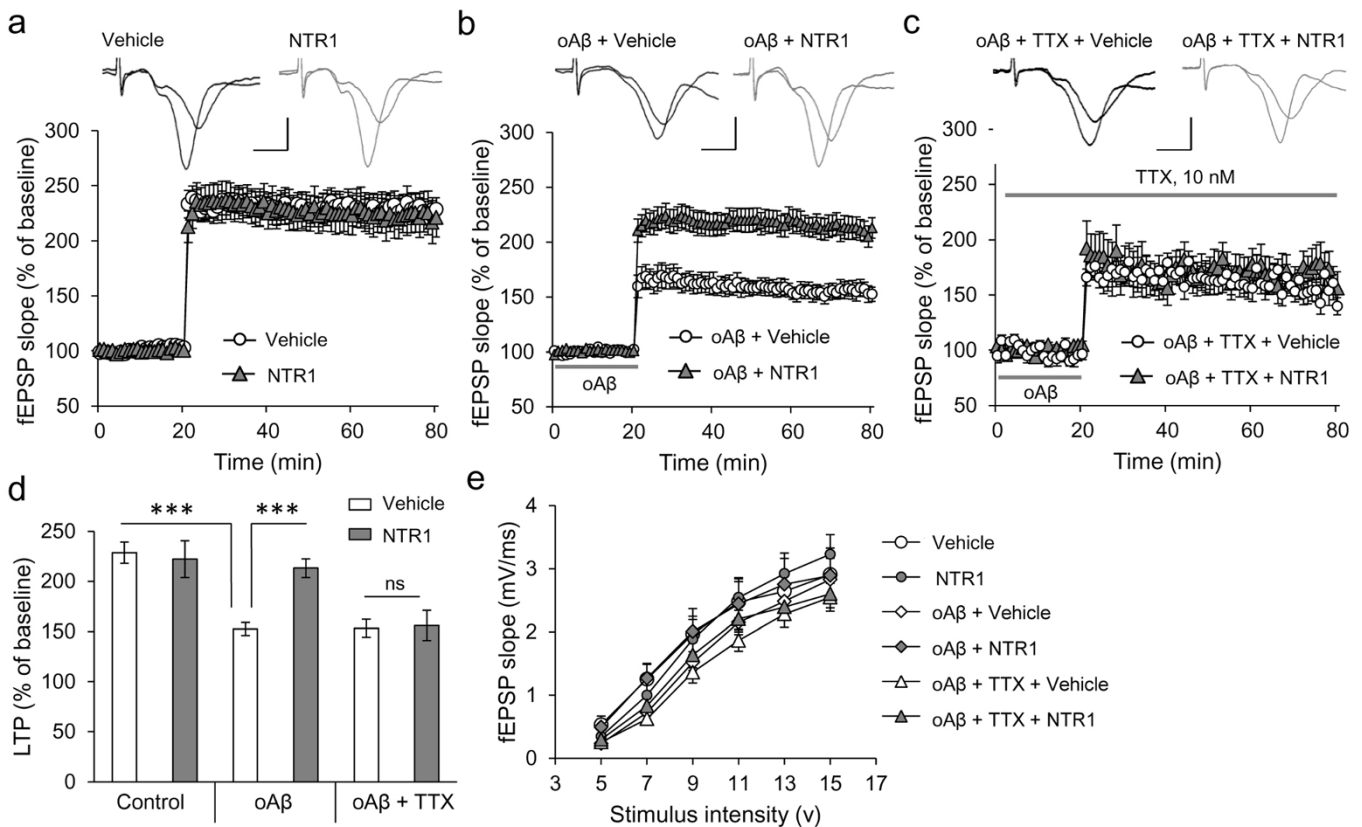


**Figure 6 | NTR1 prevents A $\beta$ 1–42 oligomers-induced hippocampal LTP reduction through a neuronal activity-dependent mechanism.** (a). NTR1 alone doesn't affect LTP. (b). NTR1 rescued oligomeric A $\beta$ 1–42-induced LTP decline. (c). Pharmacological suppression of spontaneous firing with 10 nM TTX abolishes the protective effect of NTR1 against oligomeric A $\beta$ 1–42-induced LTP impairment. Representative traces of fEPSPs before and 60 min after LTP induction with vehicle (black) or NTR1 treatment (gray) are shown in upper panel. The gray bar indicates A $\beta$ 1–42 oligomers perfusion for 20 min before TBS or TTX perfusion during whole recording. (d). Residual potentiation of fEPSPs during the last five minutes of the one hour recording. (e). Unchanged basal neurotransmission at hippocampal SC-CA1 synapses with indicated treatments.  $n=7–10$  slices from 3–5 mice. \*\*\*  $p<0.001$ ; ns, no significant.

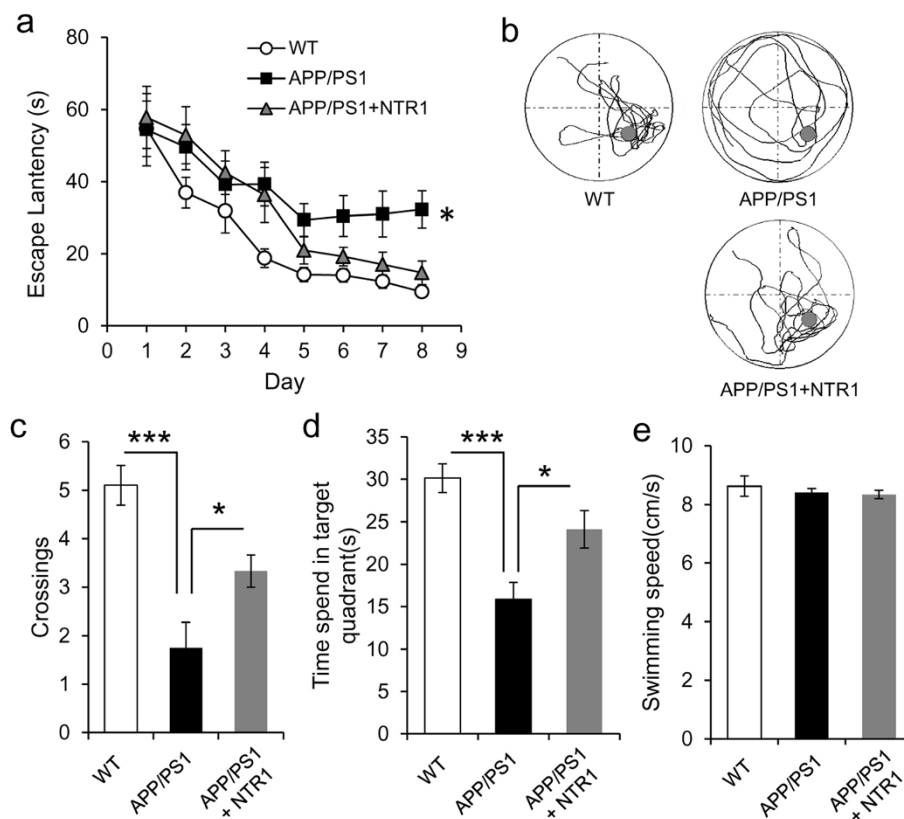


**Figure 7 | NTR1 administration ameliorates memory deficit in APP/PS1 transgenic mice.** Morris water maze test were conducted in mice with or without NTR1 ( $5 \text{ mg kg}^{-1} \text{ day}^{-1}$ , 4 months) treatment. (a). Escape latencies in hidden-platform test. (b). Representative swimming paths during the probe trial. (c). Numbers of crossings from the previous platform location. (d). Time spent in target quadrant during the probe trial. (e). The swimming speeds of mice were similar in all groups. \* $p < 0.05$ ,  $n = 8-10$  mice for each group.

silent and hyperactive neurons in AD cortex<sup>12</sup>, suggesting that a disturbance in the equilibrium between silent and hyperactive neurons, rather than an overall decrease in synaptic activity, contributes to the synaptic dysfunction in AD. These findings suggest that modulation of intrinsic properties of individual neurons is a potential strategy for preventing and/or halting AD progression. In the present study, we found that NTR1, a saponin isolated from *Panax notoginseng*, increased spontaneous firing rate in hippocampal pyramidal neurons in a reversible manner without affecting resting membrane potential or action potential amplitude. Analysis of evoked action potentials elicited with a depolarizing current injection showed a lower spike threshold in NTR1-treated pyramidal neurons, suggesting that NTR1 increases the membrane excitability of hippocampal pyramidal neurons. NTR1 has no significant effect on the maximum firing rate of hippocampal neurons, in consistent with the effect on AHP, which is known to be involved in delaying the subsequent firing of action potentials during high frequency firing<sup>41</sup>. These findings suggest that NTR1 might have the capacity of increasing neuronal excitability without resulting in hyperactivity. This advantage of NTR1 on modulation of neuronal excitability is very important because hyperactive neurons with more frequency firing are known to increase the risk of seizures<sup>8,42,43</sup>.

In an attempt to investigate mechanisms underlying changes in excitability, we analyzed the neuronal voltage-gated  $\text{K}^+$  channels. An efflux of potassium or influx of chloride can hyperpolarize the cell and thus inhibit threshold from being reached. Recent research has demonstrated that changes in voltage-gated  $\text{K}^+$  channel activity play a major pathogenic role in early stages of AD<sup>44,45</sup>. Several studies have shown that A $\beta$  increased the  $\text{K}^+$  currents including fast-inactivating  $\text{K}^+$  currents (IA) and delayed rectifier  $\text{K}^+$  currents<sup>45,46</sup>. In fact, blocking specific  $\text{K}^+$  channels has been proposed as a potential strategy for the treatment

of neurodegenerative diseases<sup>44,47</sup>. Here, we found that NTR1 significantly decreased sustained  $\text{K}^+$  currents in hippocampal neurons from either brain slice or primary cultures. These results suggest that inhibition of  $\text{K}^+$  channel activity may contribute to the decrease of spike threshold and finally modulate neuronal excitability. However, further work is needed to investigate the molecular mechanism underlying the action of NTR1 on specific voltage-gated  $\text{K}^+$  channel.

Changes in intrinsic neuronal excitability by changing the function of voltage-gated ion channels can produce broader, persistent changes in synaptic strength including synaptic transmission and plasticity<sup>48</sup>. In recent years, several lines of evidence have indicated that A $\beta$ -induces synaptic dysfunction, in part, through alteration of neuronal intrinsic excitability or disruption of the modulation of intrinsic excitability in AD brains<sup>48</sup>. Soluble A $\beta$  oligomers, composed of dimers, trimers, tetramers and higher order assemblies, inhibit hippocampal long-term potentiation (LTP), a surrogate cellular model for memory and learning<sup>35,36,49</sup>. Interestingly, previous studies have shown that A $\beta$  modulates activity of a suite of ionic conductances, mostly potassium channels through amylin receptor, which resulting in aberrant neuronal excitability<sup>50,51</sup>. In addition, another independent study showed that A $\beta$ -induced depression of hippocampal long-term potentiation is associated with the amylin receptor<sup>52</sup>. These findings suggest that alternation of neuronal excitability might contribute to A $\beta$ -induced LTP impairment. In the present study, we found that the deteriorating effect of A $\beta$  on hippocampal LTP was significantly suppressed by NTR1, a drug acting onto neuronal excitability. However, when spontaneous firing activity was reduced by a low dose of TTX ( $10 \text{ nM}$ )<sup>53</sup>, the beneficial effect of NTR1 on A $\beta$ -induced LTP impairment was completely blocked. Thus it is very likely that the improvement in synaptic plasticity caused by NTR1 due to the alternation of neuronal excitability.



LTP is widely considered one of the major cellular mechanisms underlying learning and memory<sup>54</sup>. Thus, we further evaluated the effects of NTR1 on spatial memory *in vivo* in an A $\beta$ -overexpressing mouse model. Spatial memory is understood to be strongly dependent on neuronal activity in the sub-region of hippocampus<sup>38</sup>. Previous studies have indicated that a decrease in membrane excitability induced by A $\beta$  affects neuronal activity, and probably contributes to the deficits of learning and memory in AD mouse models<sup>3,7</sup>. In the present study, all mice exhibited significant, substantial reductions in their times to find the hidden platform over the training sessions in the MWM test. However, the escape latencies of APP/PS1 mice were significantly delayed compared to the control group, which suggested that A $\beta$  decreased spatial learning ability of mice. The results from the probe trial showed that the A $\beta$  overexpressing mice spent less time in the platform quadrant with less crossing times, which further indicated that AD mice display impairment of the maintenance of established memory. Most importantly, NTR1 administration for 4 months significantly improved the spatial learning performance of AD mice both during the hidden phase and the probe trial of the MWM test, suggesting that this strategy might be beneficial in the treatment of memory loss in AD.

In summary, our data clearly demonstrate that NTR1, with a capacity of modulating the excitability of hippocampal pyramidal neurons, could prevent A $\beta$ -induced synaptic dysfunction and improve hippocampal-based memory performance in an AD mouse model. Although a previous study showed that NTR1 have protective effects against cell death induced by A $\beta$ 1-42 (10 $\mu$ M) and A $\beta$ 25-35 (20  $\mu$ M) in cultured PC12 neuronal cells<sup>55</sup>, our work revealed a novel mechanism involved in modulation of neuronal excitability, which plays a critical role in the protective effects of NTR1 against A $\beta$  toxicity.

## Methods

**Animals.** C57BL/6J mice were maintained on a 12 h light/dark cycle in temperature- and humidity-controlled rooms of the animal facility of Columbia University. Male mice (3–4 month old) were used for slice preparation and electrophysiological recording. For behavioral experiments, two-month-old male APP695sw/PS1 $\Delta$ E9 C57BL/6J (APP/PS1) mice and C57BL/6J (WT) littermates were purchased from Institute of Laboratory Animal Sciences, CAMS&PUMC (Beijing, China) and housed in a standard specific-pathogen-free facility of Beijing Normal University with free access to water and rodent chow and were kept until the age of three months. APP/PS1 mice were then randomly divided into 2 groups (n = 10 mice per group): NTR1 (5 mg kg<sup>-1</sup> day<sup>-1</sup>, by gavage) treated and vehicle (sterile distilled water) treated animals. Wild type littermates (n = 10) treated with vehicle were used as a normal control. After 4 months of administration, the Morris Water Maze task was carried out to evaluate memory in mice. All the animal experiments were carried out in accordance with the guidelines approved by the Institutional Animal Care and Use Committee of Columbia University and Beijing Normal University, respectively.

**Preparation of NTR1 and A $\beta$ 1-42 oligomers.** NTR1 (C47H80O18, molecular weight 933.16, Fig. 1A), with a purity > 99.0%, was purchased from the Chinese National Institutes for Food and Drug Control (Beijing, China). NTR1 was dissolved in sterile H<sub>2</sub>O to make 1 mM stock solution and stored at -20°C.

Human A $\beta$ 1-42 oligomers were prepared from commercially available synthetic peptides (American Peptide Company, Inc., Sunnyvale, CA) as described<sup>56</sup>. Briefly, the lyophilized peptide (1 mg) was resuspended in 250  $\mu$ L cold 1,1,1,3,3,3-hexafluoro-2-propanol (HFIP, Sigma) and aliquoted in 3 polypropylene vials. After 2 hours of incubation under the hood, HFIP was removed under gentle vacuum to form a thin film of peptide. Sealed vials were then stored at -20°C. Prior to use, 14.8  $\mu$ L anhydrous DMSO (Sigma) was added to one sealed vial to obtain a pure monomeric A $\beta$ /DMSO solution that was sonicated for 10 min and then aliquoted by 1.6  $\mu$ L per vial (5 mM). Oligomeric A $\beta$ 42 was obtained by incubating an aliquot of monomeric A $\beta$ /DMSO solution in 100  $\mu$ L sterile PBS or ACSF (80  $\mu$ M) at 4°C for 24 hours.

**Preparation of mouse acute brain slice.** Coronal brain sections of 350  $\mu$ m in thickness were sectioned in a cold sucrose-based cutting solution containing (in mM): 195 sucrose, 10 NaCl, 25 NaHCO<sub>3</sub>, 25 glucose, 2.5 KCl, 1.25 NaH<sub>2</sub>PO<sub>4</sub>, 2 Na Pyruvate, 0.5 CaCl<sub>2</sub>, and 7 MgCl<sub>2</sub> (pH 7.3) using a vibratome (Leica VT1000S) as described in previous studies<sup>57,58</sup>. Slices were permitted to recover in a submerged chamber at room temperature for at least 90 min before recordings, perfused with recording solution containing (in mM): 125 NaCl, 2.5 KCl, 1.25 NaH<sub>2</sub>PO<sub>4</sub>, 25 NaHCO<sub>3</sub>, 2 CaCl<sub>2</sub>, 1 MgCl<sub>2</sub>, 25 glucose (pH 7.3) and continuously bubbled with 95% O<sub>2</sub> and 5% CO<sub>2</sub>.

**Whole-cell patch clamp studies.** Patch clamp studies in acute brain slices were performed as previously described<sup>57,58</sup>. Briefly, for patch-clamp recording in cell cultures, cover slips were transported from the incubator to the recording chamber in a cell culture dish containing recording bath solution (in mM): 119 NaCl, 5 KCl, 20 HEPES, 30 glucose, 2 CaCl<sub>2</sub>, 2 MgCl<sub>2</sub>. The osmolarity was adjusted to ~330 mOsm with sucrose and the pH adjusted to 7.3 with 10N NaOH. For patch-clamp recording in brain slices after recovery, hippocampal CA1 pyramidal neurons were patched based on their morphology and location. We acquired whole-cell patch clamp recordings by using a MultiClamp 700B amplifier and Clampex data acquisition software (Molecular Devices) at room temperature. A glass pipette of 5–8 M $\Omega$  was fabricated and filled with electrode solution (in mM): 130 Potassium-gluconate, 10 KCl, 5 HEPES, 5 MgCl<sub>2</sub>, 0.06 CaCl<sub>2</sub>, 0.6 EGTA, 2 MgATP, 0.2 Na<sub>2</sub>GTP, and 20 Phosphocreatine. The osmolarity was adjusted to 310 mOsm and the pH adjusted to 7.1 with KOH. Spontaneous action potentials (sAPs) were recorded in current-clamp mode. Cells were held at -70 mV and step currents from -50 pA to +90 pA at 20 pA intervals were injected to elicit evoked action potentials (eAPs). K<sup>+</sup> currents were recorded in the voltage-clamp mode by delivering a 300 ms voltage step to 50 mV in cells held at -70 mV in the presence of 0.5  $\mu$ M tetrodotoxin (TTX). mEPSCs were recorded in the presence of 100  $\mu$ M picrotoxin and 0.5  $\mu$ M TTX. Signals were filtered at 2 kHz, digitized at 10 kHz, stored and analyzed off-line using Clampfit 10 (Molecular Devices) and MiniAnalysis Software (Synaptosoft Version 6.0.7). In all whole-cell recordings, a hyperpolarizing test pulse was applied at the end of the recording to ensure that the series resistance did not change significantly and was less than 25 M $\Omega$ . If so, the recordings were discarded.

**Long-term potentiation (LTP) recording.** Hippocampal CA1 LTP was recorded as described previously<sup>56</sup>. Transverse hippocampal slices (400  $\mu$ m) were cut from the mouse brain and maintained in an interface chamber at 29°C and perfused with artificial cerebrospinal fluid (ACSF) continuously bubbled with 95% O<sub>2</sub> and 5% CO<sub>2</sub>. The ACSF composition in mM was: 124 NaCl, 4.4 KCl, 1 Na<sub>2</sub>HPO<sub>4</sub>, 25 NaHCO<sub>3</sub>, 2 CaCl<sub>2</sub>, 2 MgCl<sub>2</sub>, and 10 glucose. Field-excitatory post-synaptic potentials (fEPSPs) were recorded from the CA1 region of the hippocampus by placing the stimulating electrode at the level of the Schaeffer collateral fibers, whereas the recording electrode was placed in the CA1 *stratum radiatum*. Extracellular responses were acquired using Clampex Software 10.2 (Molecular Device) and a microamplifier (IE-210, Warner Instruments). Basal synaptic transmission (BST) was assayed by plotting the stimulus voltage (V) against slopes of fEPSP to generate input-output relations. For LTP experiments, a test pulse was applied every minute at an intensity that evokes a response ~35% of the maximum evoked response. LTP was induced by  $\theta$ -burst stimulation (4 pulses at 100 Hz, with the bursts repeated at 5 Hz and each tetanus including 3 ten-burst trains separated by 15 sec). Responses were recorded for 2 hours after tetanization and measured as fEPSP slope expressed as percentage of baseline. Residual potentiation was calculated by averaging the fEPSP slopes occurring over the last five minutes of the recording.

**Behavioral studies.** Spatial learning and memory were evaluated using the Morris water maze as previously described<sup>59</sup>. Briefly, in the hidden platform test, a platform was placed at the center of one quadrant and submerged 1 cm below the water level. Mice were given 2 trials per day for 8 consecutive days (day1–8). During each trial, mice were released from four semi-randomly assigned starting points and allowed to swim for 90 s. After mounting the platform, the escape latency was recorded by software. If a mouse failed to reach the platform within 90 s, it was guided to the platform. In both situation, the animals were allowed to rest on the platform for 15 sec., and were then placed in the home cage. On the day following the hidden platform test (day 9), the probe trial was performed with the platform removed. The animal was released from the opposite quadrant and allowed to swim freely for 60 s. The time spent in the target quadrant, where the platform had been located during training, and the number of platform crossing were measured. All experiments were conducted at approximately the same time of each day. Investigators were blind of mouse genotypes and treatments until the behavioral tests were finished.

**Statistics.** Data shown in the figures represent mean  $\pm$  s.e.m. Student's paired t-tests were used in all the experiments where the effect of NTR1 was tested in the same cell. Independent t-tests were used to compare different populations of cell, synapses or mouse. For comparison of firing frequency in current injection experiment, repeat-measures ANOVA was used. For comparison of LTP and escape latency in Morris Water Maze test, two-way ANOVA was used. Significance was accepted at p < 0.05.

- Ballard, C. *et al.* Alzheimer's disease. *Lancet* **377**, 1019–1031 (2011).
- Selkoe, D. J. Alzheimer's disease is a synaptic failure. *Science* **298**, 789–791 (2002).
- Kaczorowski, C. C., Sametsky, E., Shah, S., Vassar, R. & Disterhoft, J. F. Mechanisms underlying basal and learning-related intrinsic excitability in a mouse model of Alzheimer's disease. *Neurobiol Aging* **32**, 1452–1465 (2011).
- Hoxha, E., Boda, E., Montarolo, F., Parolisi, R. & Tempia, F. Excitability and synaptic alterations in the cerebellum of APP/PS1 mice. *PLoS One* **7**, e34726 (2012).
- Brown, J. T., Chin, J., Leiser, S. C., Pangalos, M. N. & Randall, A. D. Altered intrinsic neuronal excitability and reduced Na<sup>+</sup> currents in a mouse model of Alzheimer's disease. *Neurobiol Aging* **32**, 2109–2114 (2011).



6. Palop, J. J. *et al.* Aberrant excitatory neuronal activity and compensatory remodeling of inhibitory hippocampal circuits in mouse models of Alzheimer's disease. *Neuron* **55**, 697–711 (2007).
7. Yun, S. H. *et al.* Amyloid-beta1-42 reduces neuronal excitability in mouse dentate gyrus. *Neurosci Lett* **403**, 162–165 (2006).
8. Minkeviciene, R. *et al.* Amyloid beta-induced neuronal hyperexcitability triggers progressive epilepsy. *J Neurosci* **29**, 3453–3462 (2009).
9. Palop, J. J. & Mucke, L. Amyloid-beta-induced neuronal dysfunction in Alzheimer's disease: from synapses toward neural networks. *Nat Neurosci* **13**, 812–818 (2010).
10. Prvulovic, D., Van de Ven, V., Sack, A. T., Maurer, K. & Linden, D. E. Functional activation imaging in aging and dementia. *Psychiatry Res* **140**, 97–113 (2005).
11. Silverman, D. H. *et al.* Positron emission tomography in evaluation of dementia: Regional brain metabolism and long-term outcome. *Jama* **286**, 2120–2127 (2001).
12. Busche, M. A. *et al.* Clusters of hyperactive neurons near amyloid plaques in a mouse model of Alzheimer's disease. *Science* **321**, 1686–1689 (2008).
13. Martorana, A. *et al.* Dopamine D(2)-agonist rotigotine effects on cortical excitability and central cholinergic transmission in Alzheimer's disease patients. *Neuropharmacology* **64**, 108–113 (2013).
14. Sanchez, P. E. *et al.* Levitracetam suppresses neuronal network dysfunction and reverses synaptic and cognitive deficits in an Alzheimer's disease model. *Proc Natl Acad Sci U S A* **109**, E2895–2903 (2012).
15. Yang, R. H. *et al.* Dietary omega-3 polyunsaturated fatty acids improves learning performance of diabetic rats by regulating the neuron excitability. *Neuroscience* **212**, 93–103 (2012).
16. Zheng, C. S. *et al.* Computational pharmacological comparison of and used in the therapy of cardiovascular diseases. *Exp Ther Med* **6**, 1163–1168 (2013).
17. Sun, B., Xiao, J., Sun, X. B. & Wu, Y. Notoginsenoside R1 attenuates cardiac dysfunction in endotoxemic mice: an insight into oestrogen receptor activation and PI3K/Akt signalling. *Br J Pharmacol* **168**, 1758–1770 (2013).
18. Du, Q., Jerz, G., Waibel, R. & Winterhalter, P. Isolation of dammarane saponins from Panax notoginseng by high-speed counter-current chromatography. *J Chromatogr A* **1008**, 173–180 (2003).
19. Liu, W. J. *et al.* Notoginsenoside R1 attenuates renal ischemia-reperfusion injury in rats. *Shock* **34**, 314–320 (2010).
20. Zhang, W. J., Wojta, J. & Binder, B. R. Notoginsenoside R1 counteracts endotoxin-induced activation of endothelial cells in vitro and endotoxin-induced lethality in mice in vivo. *Arterioscler Thromb Vasc Biol* **17**, 465–474 (1997).
21. Zhang, H. S. & Wang, S. Q. Notoginsenoside R1 from Panax notoginseng inhibits TNF-alpha-induced PAI-1 production in human aortic smooth muscle cells. *Vascul Pharmacol* **44**, 224–230 (2006).
22. Gu, B. *et al.* Possible protection by notoginsenoside R1 against glutamate neurotoxicity mediated by N-methyl-D-aspartate receptors composed of an NR1/NR2B subunit assembly. *J Neurosci Res* **87**, 2145–2156 (2009).
23. Chen, F., Eckman, E. A. & Eckman, C. B. Reductions in levels of the Alzheimer's amyloid beta peptide after oral administration of ginsenosides. *FASEB J* **20**, 1269–1271 (2006).
24. Yang, L. *et al.* Ginsenoside Rg3 promotes beta-amyloid peptide degradation by enhancing gene expression of neprilysin. *J Pharm Pharmacol* **61**, 375–380 (2009).
25. Wang, Y. H. & Du, G. H. Ginsenoside Rg1 inhibits beta-secretase activity in vitro and protects against Abeta-induced cytotoxicity in PC12 cells. *J Asian Nat Prod Res* **11**, 604–612 (2009).
26. Li, L. *et al.* Ginsenoside Rd attenuates beta-amyloid-induced tau phosphorylation by altering the functional balance of glycogen synthase kinase 3beta and protein phosphatase 2A. *Neurobiol Dis* **54**, 320–328 (2013).
27. Huang, T. *et al.* Ginsenoside Rg1 attenuates oligomeric Abeta(1-42)-induced mitochondrial dysfunction. *Curr Alzheimer Res* **9**, 388–395 (2012).
28. Fang, F. *et al.* Multi-faced neuroprotective effects of Ginsenoside Rg1 in an Alzheimer mouse model. *Biochim Biophys Acta* **1822**, 286–292 (2012).
29. Lee, S. T., Chu, K., Sim, J. Y., Heo, J. H. & Kim, M. Panax ginseng enhances cognitive performance in Alzheimer disease. *Alzheimer Dis Assoc Disord* **22**, 222–226 (2008).
30. Petkov, V. D. & Mosharraf, A. H. Effects of standardized ginseng extract on learning, memory and physical capabilities. *Am J Chin Med* **15**, 19–29 (1987).
31. Liu, J. *et al.* Ginsenoside rd attenuates cognitive dysfunction in a rat model of Alzheimer's disease. *Neurochem Res* **37**, 2738–2747 (2012).
32. D'Amelio, M. & Rossini, P. M. Brain excitability and connectivity of neuronal assemblies in Alzheimer's disease: from animal models to human findings. *Prog Neurobiol* **99**, 42–60 (2012).
33. Kerchner, G. A. & Nicoll, R. A. Silent synapses and the emergence of a postsynaptic mechanism for LTP. *Nat Rev Neurosci* **9**, 813–825 (2008).
34. Yang, R. H. *et al.* Paradoxical sleep deprivation impairs spatial learning and affects membrane excitability and mitochondrial protein in the hippocampus. *Brain Res* **1230**, 224–232 (2008).
35. Lambert, M. P. *et al.* Diffusible, nonfibrillar ligands derived from Abeta1-42 are potent central nervous system neurotoxins. *Proc Natl Acad Sci U S A* **95**, 6448–6453 (1998).
36. Walsh, D. M. *et al.* Naturally secreted oligomers of amyloid beta protein potently inhibit hippocampal long-term potentiation in vivo. *Nature* **416**, 535–539 (2002).
37. Eichenbaum, H. The hippocampus and mechanisms of declarative memory. *Behav Brain Res* **103**, 123–133 (1999).
38. Eichenbaum, H. A cortical-hippocampal system for declarative memory. *Nat Rev Neurosci* **1**, 41–50 (2000).
39. Marcello, E., Epis, R., Saraceno, C. & Di Luca, M. Synaptic dysfunction in Alzheimer's disease. *Adv Exp Med Biol* **970**, 573–601 (2012).
40. Harris, J. A. *et al.* Transsynaptic progression of amyloid-beta-induced neuronal dysfunction within the entorhinal-hippocampal network. *Neuron* **68**, 428–441 (2010).
41. Takigawa, T. & Alzheimer, C. Interplay between activation of GIRK current and deactivation of Ih modifies temporal integration of excitatory input in CA1 pyramidal cells. *J Neurophysiol* **89**, 2238–2244 (2003).
42. Amatniek, J. C. *et al.* Incidence and predictors of seizures in patients with Alzheimer's disease. *Epilepsia* **47**, 867–872 (2006).
43. Hauser, W. A., Morris, M. L., Heston, L. L. & Anderson, V. E. Seizures and myoclonus in patients with Alzheimer's disease. *Neurology* **36**, 1226–1230 (1986).
44. Angulo, E. *et al.* Up-regulation of the Kv3.4 potassium channel subunit in early stages of Alzheimer's disease. *J Neurochem* **91**, 547–557 (2004).
45. Yu, S. P., Farhangrazi, Z. S., Ying, H. S., Yeh, C. H. & Choi, D. W. Enhancement of outward potassium current may participate in beta-amyloid peptide-induced cortical neuronal death. *Neurobiol Dis* **5**, 81–88 (1998).
46. Plant, L. D. *et al.* Amyloid beta peptide as a physiological modulator of neuronal 'A'-type K+ current. *Neurobiol Aging* **27**, 1673–1683 (2006).
47. Skaper, S. D. Ion channels on microglia: therapeutic targets for neuroprotection. *CNS Neurol Disord Drug Targets* **10**, 44–56 (2011).
48. Zhang, W. & Linden, D. J. The other side of the engram: experience-driven changes in neuronal intrinsic excitability. *Nat Rev Neurosci* **4**, 885–900 (2003).
49. Klyubin, I. *et al.* Amyloid beta protein immunotherapy neutralizes Abeta oligomers that disrupt synaptic plasticity in vivo. *Nat Med* **11**, 556–561 (2005).
50. Jhamandas, J. H. *et al.* Cellular mechanisms for amyloid beta-protein activation of rat cholinergic basal forebrain neurons. *J Neurophysiol* **86**, 1312–1320 (2001).
51. Jhamandas, J. H., Harris, K. H., Cho, C., Fu, W. & MacTavish, D. Human amylin actions on rat cholinergic basal forebrain neurons: antagonism of beta-amyloid effects. *J Neurophysiol* **89**, 2923–2930 (2003).
52. Kimura, R., MacTavish, D., Yang, J., Westaway, D. & Jhamandas, J. H. Beta amyloid-induced depression of hippocampal long-term potentiation is mediated through the amylin receptor. *J Neurosci* **32**, 17401–17406 (2012).
53. Liu, H. N. *et al.* Presynaptic activity and Ca2+ entry are required for the maintenance of NMDA receptor-independent LTP at visual cortical excitatory synapses. *J Neurophysiol* **92**, 1077–1087 (2004).
54. Bliss, T. V. & Collingridge, G. L. A synaptic model of memory: long-term potentiation in the hippocampus. *Nature* **361**, 31–39 (1993).
55. Ma, B. *et al.* Notoginsenoside R1 attenuates amyloid-beta-induced damage in neurons by inhibiting reactive oxygen species and modulating MAPK activation. *Int Immunopharmacol* **22**, 151–159 (2014).
56. Du, H. *et al.* Cyclophilin D deficiency attenuates mitochondrial and neuronal perturbation and ameliorates learning and memory in Alzheimer's disease. *Nat Med* **14**, 1097–1105 (2008).
57. Ren, H. *et al.* FoxO1 target Gpr17 activates AgRP neurons to regulate food intake. *Cell* **149**, 1314–1326 (2012).
58. Orozco, I. J., Koppensteiner, P., Ninan, I. & Arancio, O. The schizophrenia susceptibility gene DTNBP1 modulates AMPAR synaptic transmission and plasticity in the hippocampus of juvenile DBA/2J mice. *Mol Cell Neurosci* **58c**, 76–84 (2013).
59. Vorhees, C. V. & Williams, M. T. Morris water maze: procedures for assessing spatial and related forms of learning and memory. *Nat Protoc* **1**, 848–858 (2006).

## Acknowledgments

This work was financed by grants from National Natural Science Foundation of China (No.81274118, No.81230010), the Key New Drug Creation and Development Program of China (No.2012ZX09103-201) awarded to W.Z., and the China Scholarship Council awarded to S.Y. O.A. was supported by the National Institutes of Health (NS049442).

## Author contributions

S.Y. designed and conducted electrophysiological experiments, analyzed data, and wrote the article; Z.L. and H.L. conducted behavioral experiments; O.A. and W.Z. designed, analyzed data and wrote the article.

## Additional information

**Competing financial interests:** The authors declare no competing financial interests.

**How to cite this article:** Yan, S., Li, Z., Li, H., Arancio, O. & Zhang, W. Notoginsenoside R1 increases neuronal excitability and ameliorates synaptic and memory dysfunction following amyloid elevation. *Sci. Rep.* **4**, 6352; DOI:10.1038/srep06352 (2014).



This work is licensed under a Creative Commons Attribution-NonCommercial-NoDerivs 4.0 International License. The images or other third party material in this article are included in the article's Creative Commons license, unless indicated otherwise in the credit line; if the material is not included under the Creative Commons license, users will need to obtain permission from the license holder in order to reproduce the material. To view a copy of this license, visit <http://creativecommons.org/licenses/by-nc-nd/4.0/>